Research Square

Preprints are preliminary reports that have not undergone peer review.
They should not be considered conclusive, used to inform clinical practice,
or referenced by the media as validated information.

Targeting CDK7 to overcome hypomethylating agent resistance in acute myeloid leukemia

Bon-Kwan Koo
Asan Medical Center
Eun-Ji Choi
Asan Medical Center
Ju Hyun Moon
Asan Medical Center
Ji Yun Kim
Asan Medical Center
Hyunkyung Park
Asan Medical Center
Joon Young Hur
Asan Medical Center
Han-Seung Park
Asan Medical Center
Yunsuk Choi
Asan Medical Center
Jung-Hee Lee
Asan Medical Center
Je-Hwan Lee
Asan Medical Center
Eun-Hye Hur
gracehur@amc.seoul.kr

Asan Medical Center

Research Article

Keywords: Hypomethylating agent resistance, Acute myeloid leukemia, Cyclin dependent kinase 7 inhibitor

Posted Date: May 28th, 2026

DOI: https://doi.org/10.21203/rs.3.rs-9638666/v1

License: This work is licensed under a Creative Commons Attribution 4.0 International License.
Read Full License

Additional Declarations: No competing interests reported.

Abstract

Purpose

Hypomethylating agents (HMAs), such as azacitidine and decitabine, are widely used in elderly or medically unfit patients with acute myeloid leukemia (AML) or myelodysplastic syndrome (MDS). However, most patients eventually develop primary or acquired resistance, and outcomes following HMA failure remain poor, particularly in transplantation-ineligible patients. This study evaluated the efficacy of CDK7 inhibition as a therapeutic strategy to overcome HMA resistance *in vitro*.

Methods

HMA-resistant AML cell lines (MOLM/AZA-1 and MOLM/DEC-5) were generated to evaluate the therapeutic activity of the CDK7 inhibitor YPN-005. Cell viability was assessed using CellTiter-Glo assays. Western blot analysis was performed to examine dysregulation of DNA methyltransferases (DNMTs) and apoptotic markers. Cell cycle distribution and apoptosis were evaluated by flow cytometry. Transcriptomic changes were analyzed using quantitative reverse transcription polymerase chain reaction arrays.

Results

YPN-005 demonstrated potent growth-inhibitory effects in HMA-resistant cells, with efficacy comparable to that observed in parental MOLM-13 cells. Mechanistically, CDK7 inhibition reduced DNMT expression and decreased RNA polymerase II (Ser2/5/7) phosphorylation. YPN-005 significantly induced apoptosis, as evidenced by increased Annexin V positivity and activation of PARP and caspase-3. Notably, CD40 expression was markedly upregulated at the transcript and protein levels.

Conclusion

CDK7 inhibition effectively induces apoptosis in HMA-resistant AML cells by suppressing RNA polymerase II phosphorylation and downregulating aberrant DNMT expression. Furthermore, induction of CD40 suggests a potential role for CDK7 blockade in modulating immunophenotypic features. These findings support CDK7 inhibition as a promising therapeutic strategy to overcome resistance to epigenetic therapies in AML/MDS.

Introduction

Hypomethylating agents (HMAs), including azacitidine (AZA) and decitabine (DEC), are widely used as frontline therapies for patients with myelodysplastic syndromes (MDS) and represent a standard treatment option for elderly or medically unfit patients with acute myeloid leukemia (AML), particularly

when combined with venetoclax [1]. HMAs exert their antileukemic effects primarily through incorporation into DNA or RNA, leading to depletion of DNA methyltransferases (DNMTs) and subsequent reactivation of epigenetically silenced tumor suppressor genes [2]. Although HMA treatment has been shown to improve survival compared with conventional therapies in patients with higher-risk MDS or AML, most patients eventually experience relapse or develop refractory disease due to primary or acquired resistance to HMAs, which is associated with poor clinical outcomes [3, 4].

Multiple mechanisms underlying HMA resistance have been proposed, including insufficient DNMT1 depletion, alterations in nucleoside metabolism, transcriptional reprogramming, and dysregulation of apoptotic signaling pathways [5]. In particular, persistent DNMT1 expression despite drug exposure and maintenance of oncogenic transcriptional programs have been associated with therapeutic resistance and disease progression [6]. However, the molecular determinants that enable leukemic cells to maintain survival under epigenetic stress remain incompletely understood.

Cyclin-dependent kinases (CDKs) are central regulators of cell cycle progression and transcriptional regulation. Among them, CDK7 occupies a unique position by functioning as a CDK-activating kinase and as a core component of the transcription initiation machinery. CDK7 phosphorylates serine 5 and serine 7 residues within the C-terminal domain of RNA polymerase II, thereby facilitating transcription initiation and promoter clearance. Through this dual role, CDK7 integrates cell-cycle control with transcriptional output, making it a critical regulator of cellular homeostasis [7].

Aberrant CDK7 activity has been reported in multiple solid tumors and hematologic malignancies, where it is associated with aggressive disease phenotypes and poor clinical outcomes [8–10]. Preclinical studies have demonstrated that pharmacologic inhibition of CDK7 preferentially suppresses transcription of short-lived anti-apoptotic and oncogenic transcripts, leading to rapid induction of apoptosis in transcriptionally addicted cancer cells [11]. In AML, several CDK7 inhibitors, including CT7001 and SY-1365, have shown potent antileukemic activity by suppressing leukemic proliferation and reducing tumor burden in xenograft models [12, 13].

Despite these promising findings, the therapeutic relevance of CDK7 inhibition in the context of HMA resistance has not been fully defined. Given the central role of CDK7 in transcriptional regulation, its inhibition may functionally disrupt DNMT-associated transcriptional programs and restore apoptotic susceptibility in leukemic cells that have acquired resistance to epigenetic therapy. YPN-005 is a highly selective CDK7 inhibitor that has demonstrated potent antiproliferative effects in AML cell lines and primary patient-derived samples [14]. Given the urgent need for effective strategies to overcome HMA resistance, this study investigated the antileukemic activity of YPN-005 in HMA-resistant AML models. Furthermore, the molecular mechanisms underlying its therapeutic effects were examined, with a particular focus on DNMT regulation, transcriptional signaling, and apoptosis induction.

Materials and methods

Cell lines and reagents

The human AML cell line MOLM-13 was obtained from DSMZ (Germany). The HMA-resistant cell lines MOLM/AZA-1 and MOLM/DEC-5 were established as previously described [15]. All cell lines were cultured at 37°C in 5% CO_2 in RPMI-1640 medium (Thermo Fisher Scientific, Waltham, MA) supplemented with 10% (v/v) fetal bovine serum (Hyclone, Logan, UT) and 1% penicillin/streptomycin (Thermo Fisher Scientific, Waltham, MA). YPN-005 (C26H28N6O2S) was kindly provided by Yungjin Pharm.

Cell viability assay

Cell viability was assessed using the luminescent-based CellTiter-Glo system (Promega, Madison, WI) according to the manufacturer's instructions. Briefly, cells were plated at 1–3 × 10^3 cells per well in a 96-well opaque plate and incubated in complete growth medium. Cells were treated with various concentrations of YPN-005, which was prepared as a 10 mmol/L stock solution in dimethyl sulfoxide (DMSO). After 72 h of incubation, cell viability was determined by measuring luminescent signals using a VICTOR™ X Light (PerkinElmer, Waltham, MA).

Annexin V/propidium iodide (PI) staining

To quantify apoptosis, cells (1 × 10^6 per well) were seeded in 6-well plates and incubated with varying concentrations of YPN-005 for 24 h. Thereafter, cells were harvested, washed, and stained using the Annexin V-FITC apoptosis detection kit I (BD Biosciences, Franklin Lakes, NJ) according to the manufacturer's protocol. The stained cells were analyzed by flow cytometry using a FACSCanto II (Becton Dickinson, San Jose, CA), and data were acquired and processed using BD FACSDiva v8.0.2 software (Becton Dickinson, San Jose, CA).

Cell cycle assay

MOLM-13, MOLM/AZA-1, and MOLM/DEC-5 cells (1 × 10^6 cells each) were treated with YPN-005 for 24 h, fixed with 70% (v/v) ethanol, and stained with 60 μg/mL PI (Sigma, St. Louis, MO) containing 10 units/mL RNaseA (Promega, Madison, WI) for 30 min. Cellular DNA content in each cell cycle phase was analyzed using a FACSCanto II flow cytometer (Becton Dickinson, San Jose, CA). The distribution of cells in each phase of the cell cycle was calculated from DNA content histograms using FlowJo™ software.

Western blotting assay

Cells were lysed with lysis buffer (Cell Signaling Technology, Danvers, MA) supplemented with Xpert protease inhibitor cocktail solution (GenDEPOT, Barker, TX) and phosphatase inhibitor cocktail set II

(Calbiochem, EMD Biosciences, Inc., La Jolla, CA). After incubation on ice for 30 min, lysates were centrifuged at 14,000 × g for 10 min at 4 °C. Protein concentration was measured using the Bradford (Coomassie) protein assay plus kit (GenDEPOT), and absorbance at 595 nm was measured using a SpectraMax M2 Multilabel Microplate Reader (Marshall Scientific, Hampton, NH). Protein samples (10 µg) were separated by sodium dodecyl sulfate-polyacrylamide gel electrophoresis and blotted onto polyvinylidene difluoride membranes (Bio-Rad Laboratories, Hercules, CA). After blocking with 5% (w/v) non-fat dry milk powder for 30 min, the membranes were incubated with primary antibodies overnight at 4°C, followed by incubation with horseradish peroxidase–conjugated secondary antibodies (Enzo Life Sciences, Inc., Farmingdale, NY). Specific antigen-antibody complexes were detected by enhanced chemiluminescence using BioFx® Chemiluminescent Sensitive Plus HRP (SurModics. IVD. Inc., Eden Prairie, MN). The specific band was visualized using Ez-Capture ST chemiluminescence imaging system (ATTO, Japan). A detailed list of the antibodies used is provided in Supplementary Table 1.

Gene expression profiling and polymerase chain reaction (PCR) array

Total RNA was isolated from MOLM-13 cells (1×10^6 cells each) treated with 20 nM YPN-005 for 24 h using RNeasy® Plus Mini Kit (Qiagen GmbH, Hilden, Germany) according to the manufacturer's instructions. RNA concentration and purity were assessed spectrophotometrically using a NanoDrop 1000 spectrophotometer (version 3.7.1; Thermo Fisher Scientific, Waltham, MA, USA). Subsequently, 1 µg of total RNA was reverse-transcribed into cDNA using the RevertAid First Strand cDNA Synthesis Kit (Thermo Fisher Scientific, Waltham, MA, USA). Gene expression profiling was performed using RT² Profiler™ PCR Array Human Cell Death PathwayFinder (Qiagen GmbH, Germany) on a real-time PCR system, following the manufacturer's protocol. Relative gene expression levels were calculated using the ΔΔCt method and normalized to housekeeping genes included in the array. The list of genes included in the RT² Profiler PCR Array Human Cell Death PathwayFinder is provided in Supplementary Data 1.

Flow cytometric analysis of CD40 expression

To evaluate surface marker expression, MOLM-13, MOLM/AZA-1, and MOLM/DEC-5 cells (1×10^6 cells each) were treated with YPN-005 (10 or 100 nM) for 24 h. Following incubation, cells were harvested, washed with 1X phosphate-buffered saline (PBS), and incubated with anti-CD40–APC Cy7 (BioLegend, San Diego, CA) or APC-Cy7–conjugated mouse IgG1 isotype control (Becton Dickinson, San Jose, CA) according to the manufactures' instructions. After staining, cells were washed and resuspended in PBS. Data acquisition was performed using a FACSCanto II (Becton Dickinson, San Jose, CA), and results were analyzed using FlowJo™ software.

Statistical analysis

All data were obtained from at least three independent experiments and are presented as mean ± standard deviation (SD). Statistical significance was determined using the Kruskal-Wallis test followed by Dunn's multiple comparison post hoc test for nonparametric data involving more than two groups. The Spearman correlation coefficient was used to evaluate relationships between continuous variables. All statistical analyses were performed using GraphPad Prism version 5.0 (GraphPad Software, Inc., La Jolla, CA, USA). A p-value < 0.05 was considered statistically significant.

Results

CDK7 inhibition suppresses growth and reverses DNMT upregulation in HMA-resistant AML cells

To determine whether CDK7 inhibition retains antileukemic activity in HMA-resistant AML cells, the effects of YPN-005 on cell viability and RNA polymerase II (Rpb1) phosphorylation status were evaluated in parental MOLM-13 cells and resistant derivatives (MOLM/AZA-1 and MOLM/DEC-5). YPN-005 markedly reduced cell viability in a concentration-dependent manner across all three cell lines, with IC_{50} values of 0.01899, 0.01319, and 0.01491 μM in MOLM-13, MOLM/AZA-1, and MOLM/DEC-5, respectively (Fig. 1a). Consistent with its mechanism as a CDK inhibitor, YPN-005 treatment led to a marked decrease in phosphorylation of Rpb1 at Ser2, Ser5, and Ser7 (Fig. 1b).

Next, whether CDK7 inhibition modulates molecular features underlying HMA resistance was examined. As previously reported, DNMT1, DNMT3A, and DNMT3B are significantly upregulated in MOLM/AZA-1 and MOLM/DEC-5 cells, contributing to therapeutic resistance [15]. In addition, pharmacologic suppression of DNMT family has been shown to exert potent antileukemic effects by modulating the PI3K/AKT/mTOR and ERK signaling pathways [16]. Consistent with these observations, YPN-005 treatment effectively reduced DNMT expression in both HMA-resistant cell lines (Fig. 1c), along with decreased levels of phosphorylated PI3K/AKT and ERK at the protein level (Supplementary Fig. 1). These results indicate that CDK7 inhibition may directly disrupt aberrant epigenetic alterations associated with HMA resistance, thereby restoring therapeutic vulnerability in HMA-resistant AML/MDS models.

CDK7 blockade reduces cell cycle–related proteins without altering cell cycle distribution

Next, the effect of YPN-005 on cell cycle regulators and phase distribution were investigated. CDK4, in complex with D-type cyclins, initiates phosphorylation of the retinoblastoma (Rb) protein in early G1, promoting release of E2F transcription factors and activation of genes required for S phase entry [17]. Subsequently, CDK2, activated by cyclins E and A, completes Rb hyperphosphorylation and regulates the G1/S transition and S phase progression, serving as a central coordinator of DNA replication and cell cycle commitment. YPN-005 consistently decreased protein levels of CDK2 and CDK4 across all three cell lines, indicating effective suppression of key CDKs that drive G1 to S phase progression (Fig. 2a). In addition, YPN-005 reduced expression of CDK9 (Fig. 2a), a key component of the positive transcription

elongation factor b complex, which phosphorylates the C-terminal domain of RNA polymerase II to promote transcriptional elongation [18]. Interestingly, despite clear suppression of CDK2, CDK4, and CDK9 protein levels, flow cytometric analysis revealed no significant alterations in cell cycle phase distribution following YPN-005 treatment (Fig. 2b). Consistent with previous reports in parental MOLM-13 cells [14], MOLM/AZA-1 and MOLM/DEC-5 cells showed no significant changes in G1, S, or G2/M fractions. These findings suggest that the antileukemic activity of CDK7 inhibition in HMA-resistant AML may be driven by mechanisms independent of conventional cell cycle arrest, such as transcriptional stress-induced apoptosis.

CDK7 inhibition induces robust apoptosis in HMA-resistant AML cells

To determine whether the antileukemic activity of CDK7 inhibition is associated with programmed cell death, Annexin V/PI staining and immunoblotting of key apoptotic regulators were performed. YPN-005 treatment significantly increased the proportion of Annexin V-positive cells across all three AML cell lines, with nearly 90% of cells undergoing apoptosis at a concentration of 100 nM. This finding indicates that apoptotic susceptibility is preserved despite the acquisition of HMA resistance (Fig. 3a and b). Consistent with these findings, YPN-005 activated intrinsic apoptotic signaling, as evidenced by cleavage of caspase-9, caspase-3, and PARP, together with marked downregulation of the anti-apoptotic protein XIAP (Fig. 3c).

In line with previous observations of minimal cell cycle arrest upon CDK7 inhibition [14], these data indicate that YPN-005 exerts its antileukemic effects primarily through induction of apoptosis rather than cell cycle blockade. Collectively, these results demonstrate that CDK7 inhibition triggers transcription-dependent apoptotic programs in parental and HMA-resistant AML cells, underscoring apoptosis as the dominant antileukemic mechanism even in resistant states.

CD40 emerges as an upregulated transcript following CDK7 inhibition

To further investigate molecular mechanisms underlying YPN-005-induced apoptosis, quantitative reverse transcription-PCR array analysis was performed to examine transcriptional programs activated by CDK7 inhibition. In MOLM-13 cells treated with YPN-005, CD40 emerged as one of the most markedly upregulated transcripts (Supplementary Fig. 2 and Supplementary Data 2). Notably, most genes included in the apoptosis-focused panel exhibited minimal changes or were transcriptionally downregulated, indicating selective rather than global activation of apoptotic gene programs following CDK7 inhibition. CD40, a prominent member of the TNF receptor superfamily, is known to modulate immune-mediated cell death pathways, including caspase activation and NF-κB–associated stress responses [19–21]. To validate these transcriptomic findings at the protein level, flow cytometric analysis of surface CD40 expression was performed. Consistent with the mRNA data, YPN-005 treatment induced a robust increase in CD40 surface expression across all three cell lines (Fig. 4a and b). These findings suggest that CDK7 inhibition triggers distinct transcriptional regulation, including CD40 induction. The

association between apoptotic activation and CD40 upregulation indicates that CD40-mediated signaling may contribute to CDK7 inhibition–induced cell death.

Discussion

In this study, pharmacologic inhibition of CDK7 by YPN-005 retained potent antileukemic activity in HMA-resistant AML cells and overcame key resistance-associated features. Using parental MOLM-13 cells and their HMA-resistant derivatives (MOLM/AZA-1 and MOLM/DEC-5), CDK7 blockade effectively suppressed RNA polymerase II phosphorylation, reversed DNMT overexpression, and induced apoptosis, despite minimal effects on cell cycle arrest. Notably, CD40 was identified as a transcriptionally upregulated death-associated receptor following CDK7 inhibition, suggesting a previously unrecognized link between transcriptional CDK regulation and proapoptotic, immune-related signaling in AML.

Resistance to HMAs such as azacitidine and decitabine remains a major clinical challenge in AML, with known mechanisms including epigenetic reprogramming and upregulation of DNMTs, including DNMT1 and DNMT3B [15, 22]. Consistent with prior reports, MOLM/AZA-1 and MOLM/DEC-5 cells exhibited marked DNMT overexpression. The findings of this study demonstrate that CDK7 inhibition significantly attenuates DNMT expression in resistant cells, suggesting that CDK7-dependent transcriptional regulation contributes to maintenance of HMA resistance. These data support targeting transcriptional dependency to disrupt the epigenetic stability of the HMA-resistant state.

Notably, although YPN-005 reduced protein levels of multiple CDKs, including CDK2, CDK4, and CDK9, it did not induce classical cell cycle arrest. This observation is consistent with prior reports and highlights a critical distinction between biochemical suppression of cell cycle regulators and functional cell cycle blockade [14]. Instead, the data indicate that apoptosis, rather than cell cycle arrest, represents the dominant antileukemic mechanism of CDK7 inhibition. This preserved apoptotic susceptibility in HMA-resistant cells is particularly relevant, as resistance to conventional therapies is often accompanied by impaired apoptotic signaling. Mechanistically, YPN-005 triggered intrinsic apoptotic pathways, as evidenced by cleavage of caspase-9, caspase-3, and PARP, along with downregulation of XIAP, thereby lowering the apoptotic threshold even in cells with established epigenetic drug resistance.

A key novel finding of this study is the identification of CD40 as a transcriptionally upregulated target on leukemic cells following CDK7 inhibition. Primarily expressed on antigen-presenting cells, CD40 not only augments anti-tumor immune responses but also directly influences tumor cell survival through extrinsic apoptotic signaling [23–25]. While several agonistic CD40 antibodies are currently undergoing clinical evaluation, predominantly in solid tumors to enhance antigen presentation and T-cell activation, their efficacy in hematologic malignancies remains poorly defined. Notably, as CDK7 inhibition directly induces CD40 upregulation on leukemic cells, this approach may synergistically enhance T-cell mediated immunity while simultaneously promoting direct leukemic cell death. These findings suggest that CDK7-targeted therapy reprograms tumor cells toward a CD40-enriched state, thereby creating a potential therapeutic window for CD40-directed immunomodulatory interventions.

Taken together, these results establish CDK7 inhibition as a promising therapeutic strategy in HMA-resistant AML by simultaneously targeting transcriptional addiction, reversing epigenetic resistance features, and inducing apoptosis through intrinsic pathways and CD40-associated signaling. These findings provide a strong preclinical rationale for further investigation of CDK7 inhibitors in patients with HMA-refractory AML/MDS.

Declarations

Competing interests

The authors have no competing interests to declare that are relevant to the content of this article.

Author Contribution

B. Koo, E. Choi, and E. Hur; Data collection: B. Koo, J.H. Moon, and J.Y. Kim; Formal analysis: H. Park, H. Park, J.Y. Hur, Y. Choi, and J. Lee; Supervision: J. Lee; Writing: B. Koo, E. Choi, and E. Hur. All authors have read and approved the final version of the manuscript.

Acknowledgement

This study was supported by a grant (ICKSH-2022-07) form the Korean Society of Hematology. We thank the R&D Institute at Yungjin Pharmaceutical Co., Ltd., for providing YPN-005.

Data Availability

All data supporting the findings of this study are available within the paper and its Supplementary Information. The list of genes included in the RT² Profiler PCR Array Human Cell Death Pathway Finder is provided in Supplementary Data 1, and the corresponding PCR array expression data are provided in Supplementary Data 2.

References

1. Estey EH. Epigenetics in clinical practice: the examples of azacitidine and decitabine in myelodysplasia and acute myeloid leukemia. Leukemia. 2013;27(9):1803–12.
2. Tsai CT, Yang PM, Chern TR, Chuang SH, Lin JH, Klemm L, et al. AID downregulation is a novel function of the DNMT inhibitor 5-aza-deoxycytidine. Oncotarget. 2014;5(1):211–23.
3. Qin T, Jelinek J, Si J, Shu J, Issa JP. Mechanisms of resistance to 5-aza-2'-deoxycytidine in human cancer cell lines. Blood. 2009;113(3):659–67.

4. Sripayap P, Nagai T, Uesawa M, Kobayashi H, Tsukahara T, Ohmine K, et al. Mechanisms of resistance to azacitidine in human leukemia cell lines. Exp Hematol. 2014;42(4):294–306.e2.
5. Stomper J, Rotondo JC, Greve G, Lübbert M. Hypomethylating agents (HMA) for the treatment of acute myeloid leukemia and myelodysplastic syndromes: mechanisms of resistance and novel HMA-based therapies. Leukemia. 2021;35(7):1873–89.
6. Gu X, Tohme R, Tomlinson B, Sakre N, Hasipek M, Durkin L, et al. Decitabine- and 5-azacytidine resistance emerges from adaptive responses of the pyrimidine metabolism network. Leukemia. 2021;35(4):1023–36.
7. Diab S, Yu M, Wang S. CDK7 Inhibitors in Cancer Therapy: The Sweet Smell of Success? J Med Chem. 2020;63(14):7458–74.
8. Huang JR, Qin WM, Wang K, Fu DR, Zhang WJ, Jiang QW, et al. Cyclin-dependent kinase 7 inhibitor THZ2 inhibits the growth of human gastric cancer in vitro and in vivo. Am J Transl Res. 2018;10(11):3664–76.
9. Wang C, Jin H, Gao D, Wang L, Evers B, Xue Z, et al. A CRISPR screen identifies CDK7 as a therapeutic target in hepatocellular carcinoma. Cell Res. 2018;28(6):690–2.
10. Zhou Y, Lu L, Jiang G, Chen Z, Li J, An P, et al. Targeting CDK7 increases the stability of Snail to promote the dissemination of colorectal cancer. Cell Death Differ. 2019;26(8):1442–52.
11. Cayrol F, Praditsuktavorn P, Fernando TM, Kwiatkowski N, Marullo R, Calvo-Vidal MN, et al. THZ1 targeting CDK7 suppresses STAT transcriptional activity and sensitizes T-cell lymphomas to BCL2 inhibitors. Nature Communications. 2017;8(1):14290.
12. Clark K, Ainscow E, Peall A, Thomson S, Leishman A, Elaine S, et al. CT7001, a Novel Orally Bio-Available CDK7 Inhibitor, Is Highly Active in in-Vitro and in-Vivo Models of AML. Blood. 2017;130:2645.
13. Hu S, Marineau JJ, Rajagopal N, Hamman KB, Choi YJ, Schmidt DR, et al. Discovery and Characterization of SY-1365, a Selective, Covalent Inhibitor of CDK7. Cancer Research. 2019;79(13):3479–91.
14. Koo BK, Choi EJ, Hur EH, Moon JH, Kim JY, Park HS, et al. Antileukemic activity of YPN-005, a CDK7 inhibitor, inducing apoptosis through c-MYC and FLT3 suppression in acute myeloid leukemia. Heliyon. 2022;8(10):e11004.
15. Hur EH, Jung SH, Goo BK, Moon J, Choi Y, Choi DR, et al. Establishment and characterization of hypomethylating agent-resistant cell lines, MOLM/AZA-1 and MOLM/DEC-5. Oncotarget. 2017;8(7):11748–62.
16. Choi EJ, Koo BK, Hur EH, Moon JH, Kim JY, Park HS, et al. Inhibition of DNMT3B and PI3K/AKT/mTOR and ERK Pathways as a Novel Mechanism of Volasertib on Hypomethylating Agent-Resistant Cells. Biomol Ther (Seoul). 2023;31(3):319–29.
17. Otto T, Sicinski P. Cell cycle proteins as promising targets in cancer therapy. Nat Rev Cancer. 2017;17(2):93–115.

18. Fu J, Yoon HG, Qin J, Wong J. Regulation of P-TEFb elongation complex activity by CDK9 acetylation. Mol Cell Biol. 2007;27(13):4641–51.
19. Natoli G, Costanzo A, Ianni A, Templeton DJ, Woodgett JR, Balsano C, et al. Activation of SAPK/JNK by TNF receptor 1 through a noncytotoxic TRAF2-dependent pathway. Science. 1997;275(5297):200–3.
20. Rothe M, Sarma V, Dixit VM, Goeddel DV. TRAF2-mediated activation of NF-kappa B by TNF receptor 2 and CD40. Science. 1995;269(5229):1424–7.
21. Tsukamoto N, Kobayashi N, Azuma S, Yamamoto T, Inoue J. Two differently regulated nuclear factor kappaB activation pathways triggered by the cytoplasmic tail of CD40. Proc Natl Acad Sci U S A. 1999;96(4):1234–9.
22. Solly F, Koering C, Mohamed AM, Maucort-Boulch D, Robert G, Auberger P, et al. An miRNA-DNMT1 Axis Is Involved in Azacitidine Resistance and Predicts Survival in Higher-Risk Myelodysplastic Syndrome and Low Blast Count Acute Myeloid Leukemia. Clin Cancer Res. 2017;23(12):3025–34.
23. Tong AW, Stone MJ. Prospects for CD40-directed experimental therapy of human cancer. Cancer Gene Ther. 2003;10(1):1–13.
24. Yan C, Richmond A. Hiding in the dark: pan-cancer characterization of expression and clinical relevance of CD40 to immune checkpoint blockade therapy. Mol Cancer. 2021;20(1):146.
25. Elgueta R, Benson MJ, de Vries VC, Wasiuk A, Guo Y, Noelle RJ. Molecular mechanism and function of CD40/CD40L engagement in the immune system. Immunol Rev. 2009;229(1):152–72.

Figures

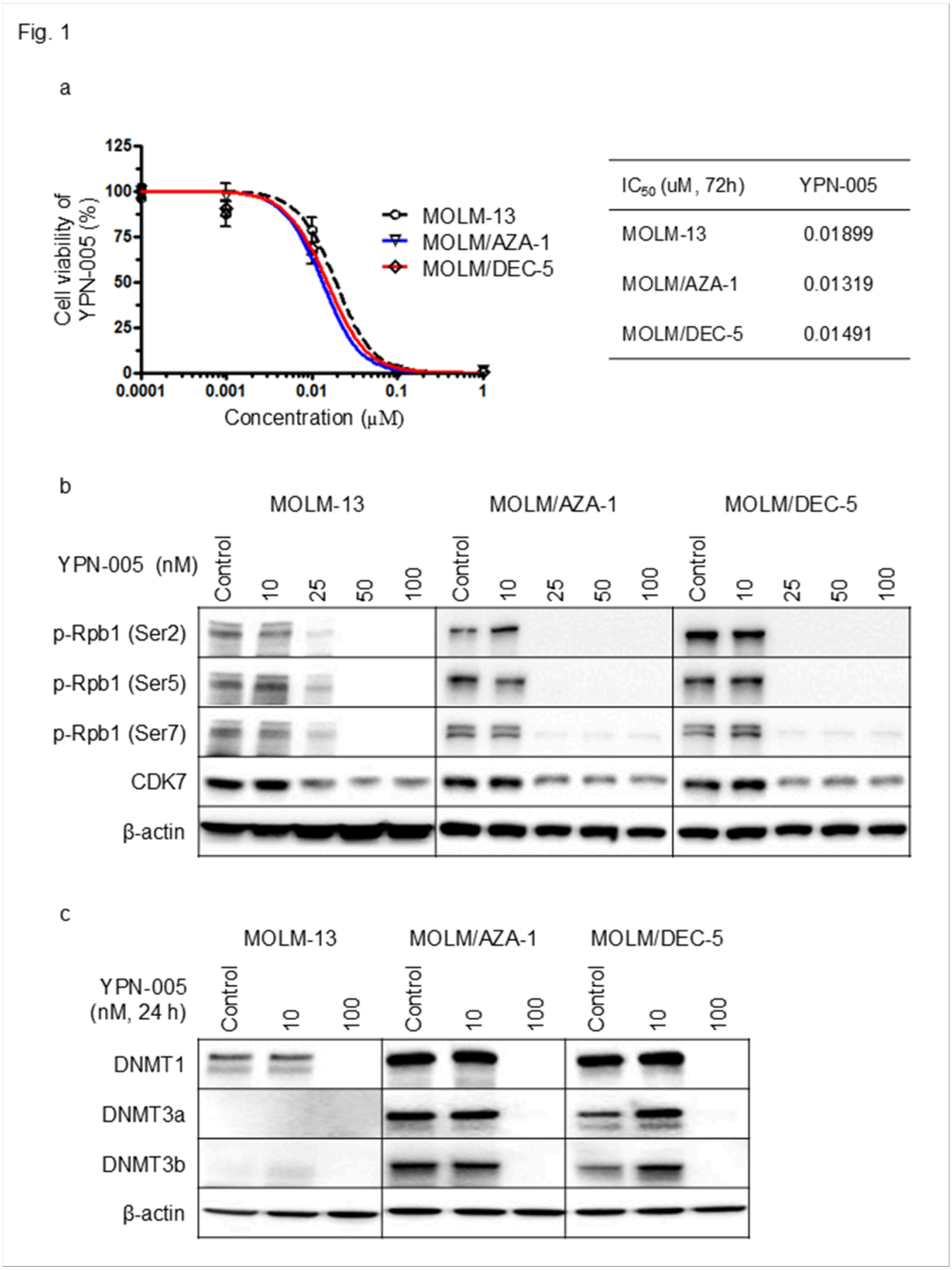


Figure 1

CDK7 inhibition leads to growth inhibition and reverses DNMT upregulation in HMA-resistant AML cells.

(a) Dose–response curves of MOLM-13, MOLM/AZA-1, and MOLM/DEC-5 cells treated with increasing concentrations of YPN-005 for 72 h. Cell viability was assessed using the CellTiter-Glo assay and

normalized to vehicle control. The table on the right summarizes calculated IC_{50} values for each cell line.

(b) Western blot analysis of phosphorylated RNA polymerase II C-terminal domain (p-Rpb1 Ser2, Ser5, and Ser7) in MOLM-13, MOLM/AZA-1, and MOLM/DEC-5 cells following YPN-005 treatment. Cells were exposed to DMSO or 10, 25, 50, or 100 nM YPN-005 for 24 h. β-actin was used as a loading control.

(c) Western blot analysis of DNA methyltransferase expression in MOLM-13, MOLM/AZA-1, and MOLM/DEC-5 cells following YPN-005 treatment. Cells were treated with YPN-005 for 24 h, and whole cell lysates were analyzed for DNMT1, DNMT3A, and DNMT3B expression levels. β-actin was used as a loading control.

Abbreviations: AML, acute myeloid leukemia; AZA, azacitidine; CDK, cyclin-dependent kinase; DMSO, dimethyl sulfoxide; DNMT, DNA methyltransferase; HMA, hypomethylating agent.

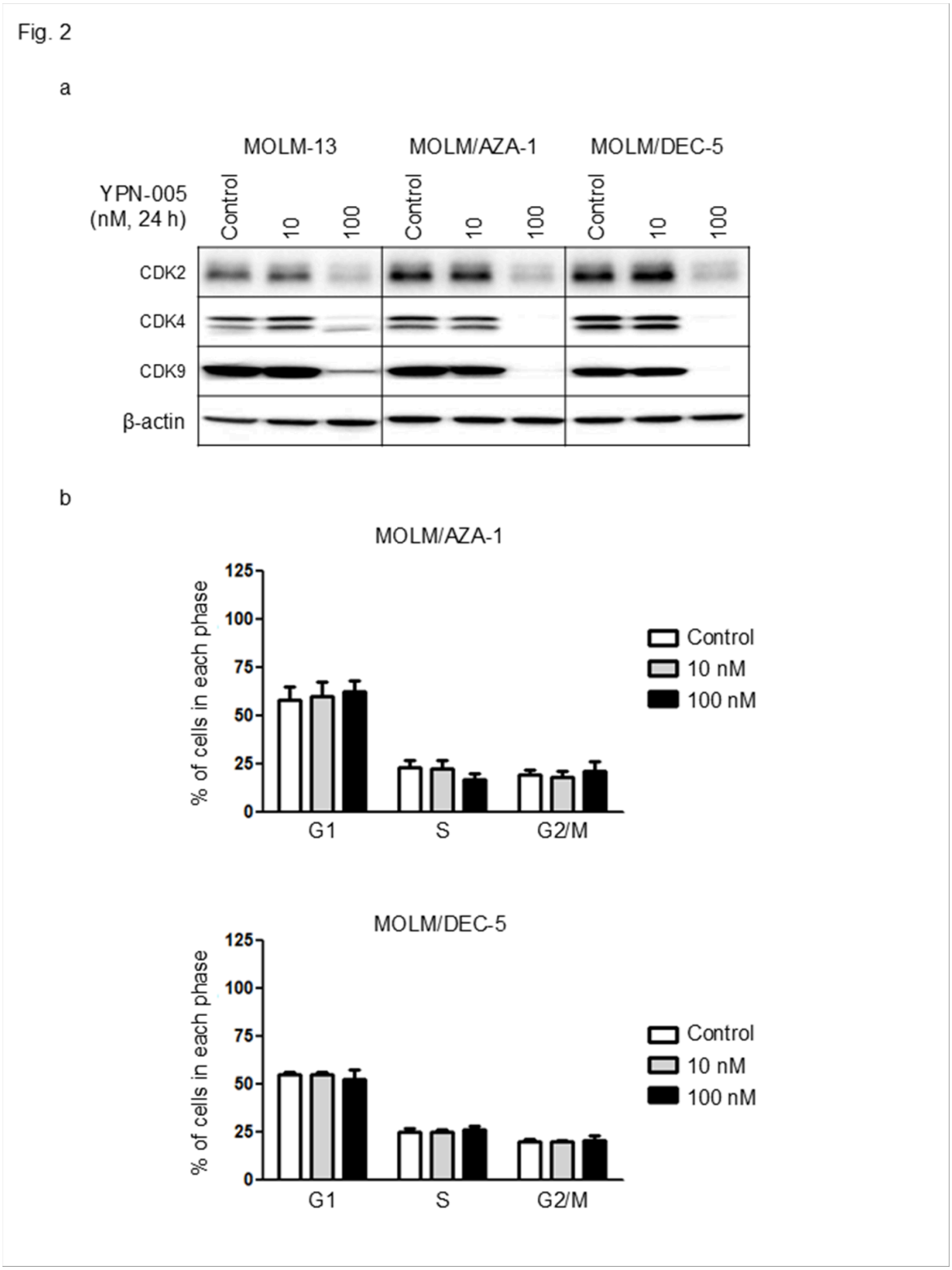


Figure 2

CDK7 blockade reduces cell cycle-related proteins without altering cell cycle distribution.

(a) Western blot analysis of cell cycle–related proteins in MOLM-13, MOLM/AZA-1, and MOLM/DEC-5 cells following YPN-005 treatment. Cells were exposed to DMSO, 10 nM, or 100 nM YPN-005 for 24 h,

and whole-cell lysates were analyzed for CDK2, CDK4, and CDK9 expression levels. β-actin served as a loading control.

(b) Cell cycle distribution following YPN-005 treatment in parental and HMA-resistant AML cells. MOLM-13, MOLM/AZA-1, and MOLM/DEC-5 cells were treated with DMSO, 10 nM, or 100 nM YPN-005 for 24 h, stained with PI, and analyzed by flow cytometry.

Abbreviations: AML, acute myeloid leukemia; CDK, cyclin-dependent kinase; DMSO, dimethyl sulfoxide; HMA, hypomethylating agent; PI, propidium iodide.

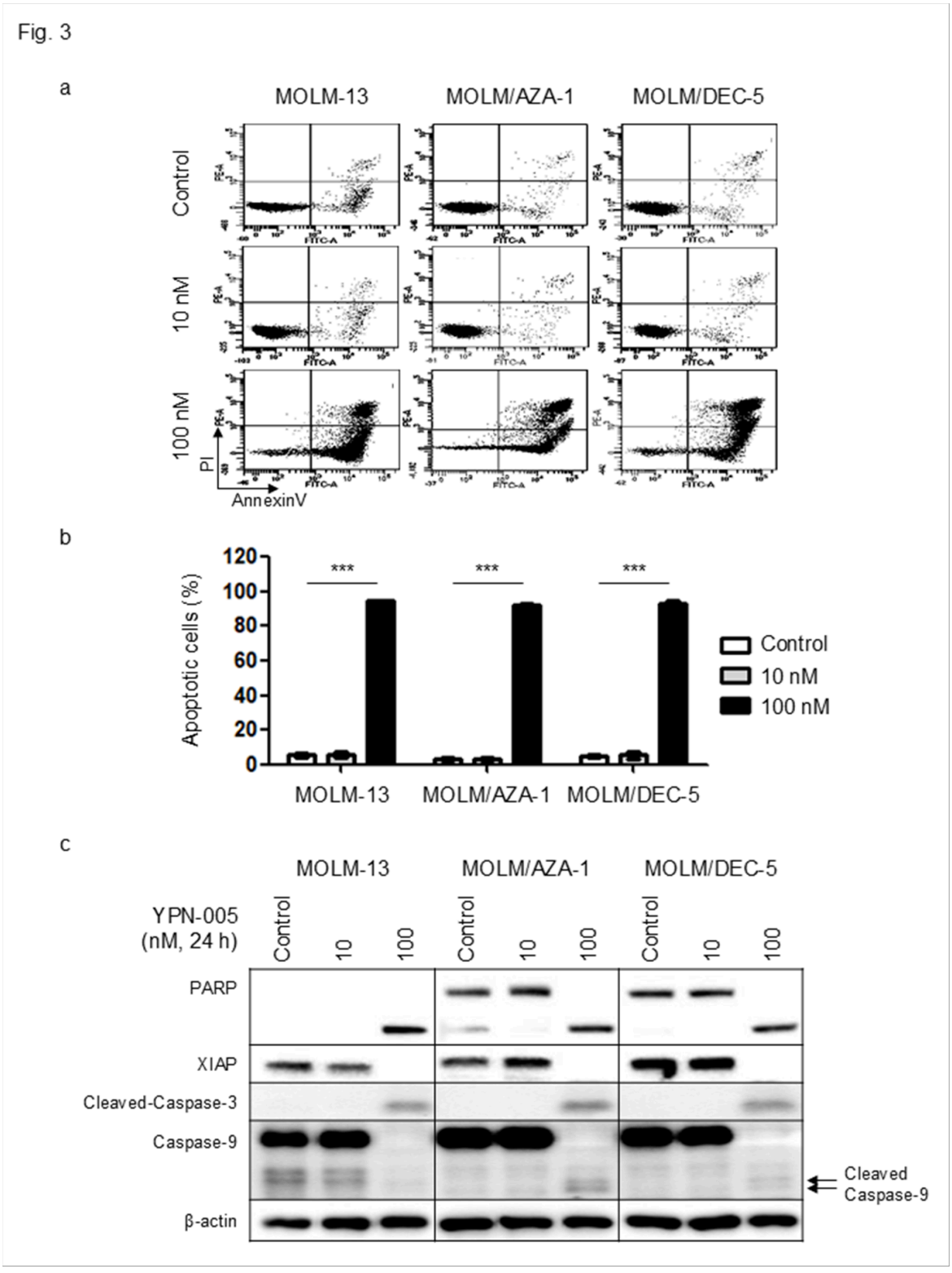


Figure 3

CDK7 inhibition induces robust apoptosis in parental and HMA-resistant AML cells.

(a) Representative flow cytometric dot plots of Annexin V-FITC/PI staining in MOLM-13, MOLM/AZA-1, and MOLM/DEC-5 cells following YPN-005 treatment. Cells were exposed to DMSO, 10 nM, or 100 nM YPN-005 for 24 h and analyzed for apoptotic populations.

(b) Quantification of apoptotic cells in parental and HMA-resistant AML cells. Bar graphs represent the percentage of total apoptotic cells. *$p < 0.001$ compared with DMSO.

(c) Western blot analysis of apoptosis-related markers following YPN-005 treatment in parental and HMA-resistant AML cells. Whole-cell lysates collected after 24 h exposure were probed for cleaved PARP, XIAP, cleaved caspases-3, and cleaved caspase-9. β-actin served as a loading control. Arrows indicate cleaved forms of the respective proteins.

AML, acute myeloid leukemia; DMSO, dimethyl sulfoxide; FITC, fluorescein isothiocyanate; HMA, hypomethylating agent; PI, propidium iodide.

Fig. 4

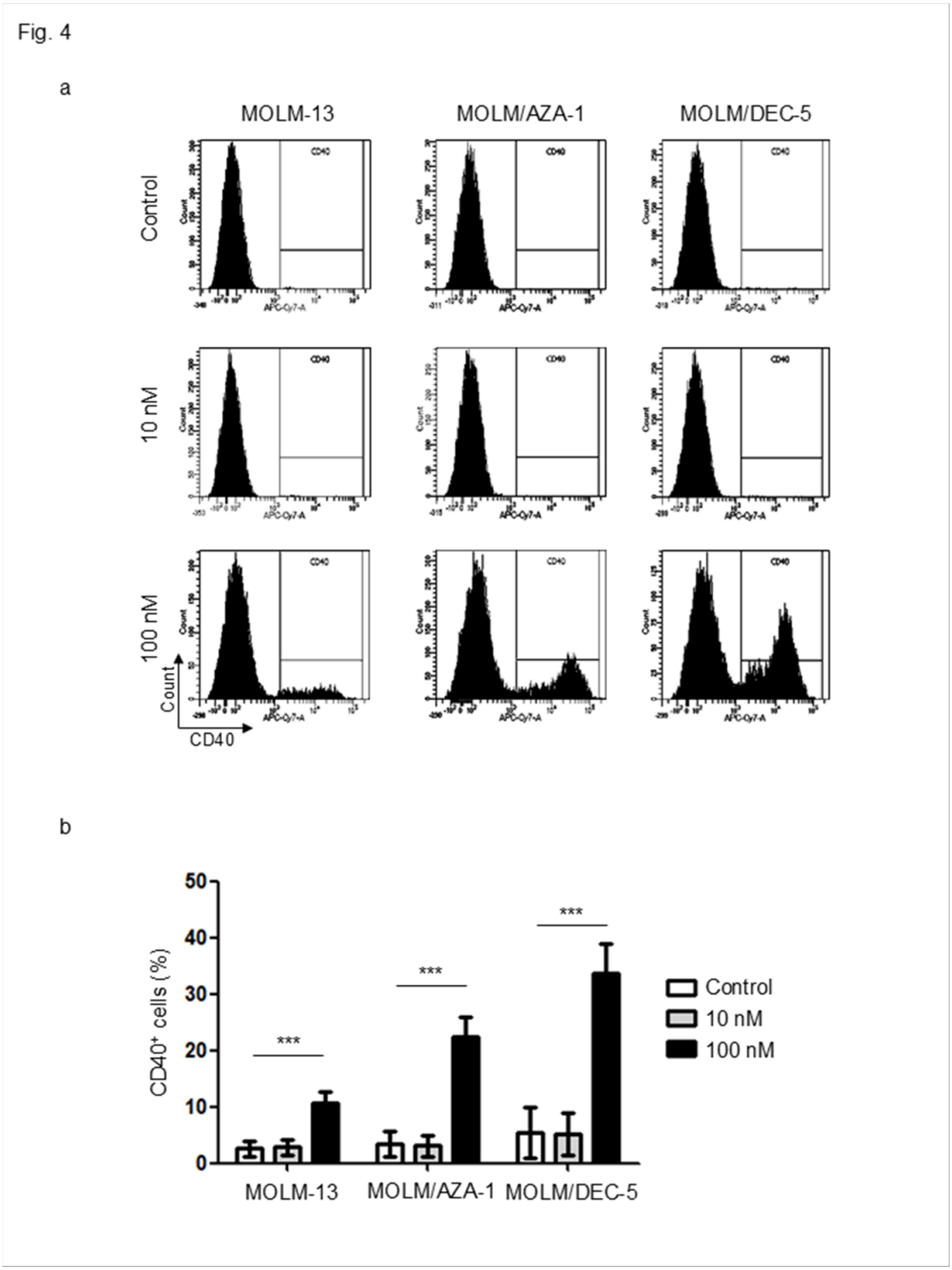


Figure 4

CD40 emerges as an upregulated transcript following CDK7 inhibition.

(a) Representative flow cytometry histograms showing CD40 surface expression in MOLM-13, MOLM/AZA-1, and MOLM/DEC-5 cells following YPN-005 treatment. Cells were exposed to DMSO, 10 nM, or 100 nM YPN-005 for 24 h and stained with anti-CD40 antibody.

(b) Quantification of CD40-positive cell populations from three independent experiments. Bar graphs represent the percentage of CD40-expressing cells in each treatment group. ***$p < 0.001$ compared with DMSO.

DMSO, dimethyl sulfoxide.

Supplementary Files

This is a list of supplementary files associated with this preprint. Click to download.

- CDK7iinHMARSupplementaryTableandFigureF.docx
- CDK7iinHMARSupplementaryData1PCRArraygenelistF.xlsx
- CDK7iinHMARSupplementaryData2PCRArrayresultF.xlsx
- Figure1cFulluncroppedblots.tif
- SupplementaryFigure12Fulluncroppedblots.tif
- Figure2aFulluncroppedblots.tif
- Figure1bFulluncroppedblots.tif
- Figure3cFulluncroppedblots.tif
- SupplementaryFigure11Fulluncroppedblots.tif
- SupplementaryFigure14Fulluncroppedblots.tif
- SupplementaryFigure13Fulluncroppedblots.tif